Available online at www.ijpcr.com
International Journal of Pharmaceutical and Clinical Research 2016; 8(8): 1205-1211

ISSN- 0975 1556

Research Article

Analogue and Structure Based Drug Designing of Prenylated Flavonoid Derivatives as PKB/Akt1 Inhibitors

Neelamma M[1], Anuradha G H[2], Shravan Kumar Gunda[3*]

[1]*Department of Chemistry, University College of Science, Saifabad, Hyderabad, Telangana State, India*
Sardar Patel College, Osmania University, Secunderabad, Telangana
[2]*Division of Bioinformatics, Osmania University, Hyderabad, Telangana State, India*

Available Online:10th August, 2016

ABSTRACT

The 3D-QSAR studies on prenylated flavonoid derivatives as PKB/Akt1 inhibitors were endeavored using CoMFA and CoMSIA studies. Internal and external validation techniques were investigated using leave-one-out, no-validation and cross-validation and bootstrapping. The CoMFA model predicted satisfactory correlation coefficient q^2 value of 0.880 and conventional correlation coefficient r^2 value of 0.973, while CoMSIA model predicted q^2 value of 0.906 and r^2 value of 0.991, inferring the important role of steric and electrostatic properties of candidate compounds. The models were graphically interpreted by using contour plots, which gave more accuracy into the structural requirements for increasing the biological activity of compounds and proved a strong basis for future rational drug design of more active inhibitors for cancer. The resulting CoMFA and CoMSIA contour map analysis were used to classify the structural features relevant to the biological activity in selected series of prenylated flavonoid derivatives. Molecular docking studies were also carried out for all 56 PKB/Akt1 inhibitors in the binding pocket of "Akt1 with AMP-PNP" (PDB id: 4EKK). The results revealed that these derivatives act as anti-cancer agents.

Keywords: Prenylated flavonoids, PKB/Akt1 inhibitors, Cancer, CoMFA, CoMSIA, Autodock

INTRODUCTION

Protein kinase B also known as Akt. It is located downstream in the PI-3 (phosphatidylinositol-3-kinase) kinase pathway and also play pivotal role in the balance of cellular survival and apoptosis[1]. It is a serine/threonine kinase belongs to the AGC family of kinases[2]. It plays important role in signal transduction pathways. In mammals PKB is comprised of 3 highly homologous isoforms, viz., (1) PKBα, (2) PKBβ, and (3) PKBγ[3]. Inhibitors of protein kinase B are useful agents for the treatment of cancer. Phosphorylation at serine and threonine is accompanied by the activation of Akt kinases[4]. Recent studies show that PKB plays a major role in cancer progression by stimulating cell proliferation and inhibiting apoptosis[5]. In general, the 3D-QSAR techniques are valuable methods of analogue-based drug design by correlating physicochemical properties from a set of related compounds to their known molecular property or molecular activity values. The present investigation reports the first application of 3D-QSAR to study of Prenylated flavonoid derivatives as potent anticancer PKB/AKT1 inhibitors. We studied fifty-six Prenylated flavonoid derivatives as PKB/AKT1 inhibitors using CoMFA (comparative molecular field analysis)[6] and CoMSIA (comparative molecular similarity indices analysis)[7]. Models obtained from 3D-QSAR studies provide a strong basis for future rational design of more active and selective PKB/AKT1 receptor agonists. Molecular docking studies were also performed for all the 56 inhibitors by taking co-crystal structure from PDB (protein data bank).

MATERIALS AND METHODS

Data Set

In this study, a dataset of 56 compounds obtained from the literature[8] consisted of prenylated flavonoid derivatives showed inhibitory activity towards PKB/Akt1 receptor. In a total set of 56 compounds reported, 47 compounds were used as training set and 9 compounds were used as test set based on random selection. The pIC_{50} values of these compounds range from 4.49 to 8.82 providing a wide range and homogenous data set for 3D-QSAR study. For QSAR analysis, the given IC_{50} values

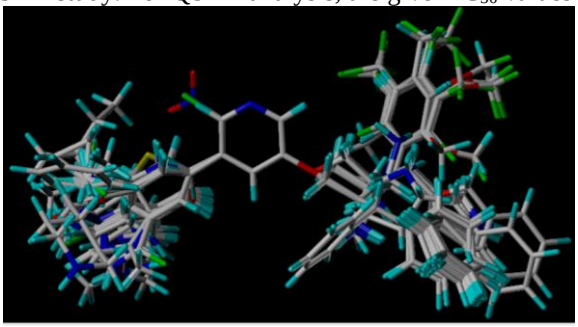

Figure 1: Atom based alignment of prenylated flavonoids as PKB/AKT1 inhibitors superimposed on template molecule (4)

**Author for Correspondence: gunda14@gmail.com*

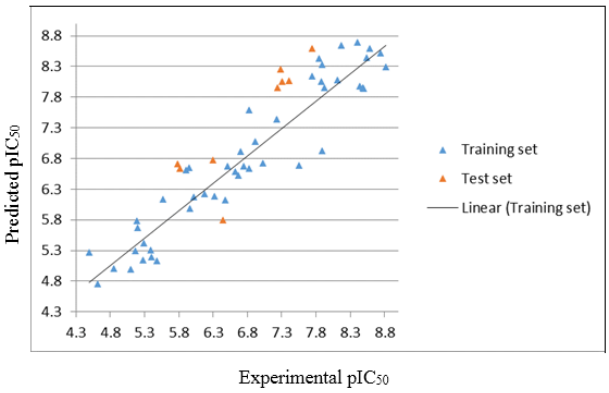

2(a)

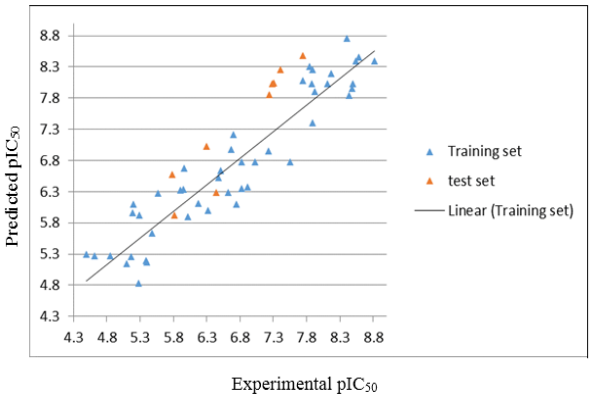

2(b)

Figure 2: Experimental versus predicted activities of CoMFA and CoMSIA analysis

Table 1: Statistical Analysis of CoMFA and CoMSIA models

	CoMFA		CoMSIA	
q^2	0.880		0.906	
r^2	0.973		0.991	
SEE	0.225		0.134	
F value	293.248		700.295	
CV	0.883		0.910	
Bootstrap	Mean	Std.dev	Mean	Std.dev
SEE	0.186	0.102	0.111	0.710
r^2	0.980	0.007	0.993	0.003
Field Contribution (%)				
Steric	55.3		9.20	
Electrostatic	49.7		23.1	
Hydrophobic			15.7	
Donor			32.3	
Acceptor			19.7	

were changed to minus logarithmic scale value (pIC_{50})[9] as a dependent variable and molecular descriptors as independent variable for CoMFA and CoMSIA analysis. The pIC_{50} values of these compounds range from 4.49 to 8.82 providing a wide range and homogenous data set for 3D-QSAR study.

$pIC_{50} = -\log(IC_{50})$.

The structures of prenylated flavonoids and their biological activities of all compounds including both training set and test set molecules is shown in Table 1 and Table 2. Compound structures are shown in table 4.

Structure building and minimization

Structures of all the molecules were sketched in SYBYL 6.7. Energy minimization was performed on each prenylated flavonoid derivative using Tripos force field with distance-dependent dielectric function and powell conjugate gradient algorithm with a convergence gradient of 0.005 kcal/mol, all the molecules were minimized by adding Gasteiger-Huckel charges[10]. The compound 4 with the least IC_{50} (highest pIC_{50}) value was utilized as a template. The common scaffold of every inhibitor occupies the same area in 3D space. The most active compound was used as the reference compound to align all the compounds using atom-to-atom matching.

Molecular alignment

Molecular alignment plays an important role in CoMFA and CoMSIA methods and their results are extremely sensitive to a number of factors like alignment rule and orientation rule of the aligned 56 compounds, probe atom type and lattice shifting step size. The most active compound (compound 4) was used as the scaffolds for aligning rest of the molecules by default SYBYL align database option. The structures of aligned molecules are shown in Fig. 1

3D-QSAR studies

Comparative molecular field analysis has been used extensively to relate the chemical structure to their biological properties. Comparative molecular field analysis fields are interaction energies between molecule and a set of aligned molecules or a probe, which are used to establish the 3D-QSAR equations. The steric and electrostatic field potentials for CoMFA were calculated at each lattice intersection of a regularly spaced grid of 2.0 Å which provides all information necessary for understanding the biological properties of a set of compounds. The Van der Waals potential and columbic terms, which represent steric and electrostatic fields, respectively, were calculated using Tripos force field[11]. The steric and electrostatic interaction energies were calculated for each molecule at each grid point using a sp^3 carbon probe with a +1.0 charge. An energy cut off value of 30 kcal/mol was imposed on all CoMFA calculations to avoid excessively high and unrealistic energy values within the molecule. With standard option for the scaling of variables, the regression analysis was carried out using cross-validated partial least squares approach (PLS) of LOO (leave-one-out). After that a non-cross-validated analysis was carried out without column filtering.

CoMFA studies

Steric and electrostatic properties were calculated using Tripos force field engine and the aligned molecules were placed in a 3D grid box so that the entire set was included. CoMFA descriptors were generated using sp^3 probe atom carrying +1 charge to generate steric and electrostatic fields. 30 kcal/mol cut-off was used for the analysis and standard options were used for the calculation of regression analysis. Partial least square (PLS) was done by selecting leave-one-out (LOO) using 5 as the number of components and the column filtering was set as 2.0 kcal/mol.

CoMSIA studies

CoMSIA study was performed with the QSAR option in

Table 2: Experimental, predicted and residual values training set compounds of CoMFA, CoMSIA study

S. No.	pIC_{50}	CoMFA		CoMSIA	
		Predicted	Residual	Predicted	Residual
1	8.74	8.52	0.22	9.19	-0.45
2	8.54	8.44	0.10	8.39	0.15
3	8.58	8.60	-0.02	8.45	0.13
4	8.82	8.29	0.53	8.39	0.43
5	8.41	8.69	-0.28	8.76	-0.35
7	7.88	8.05	-0.17	8.03	-0.15
8	7.74	8.14	-0.40	8.08	-0.34
9	8.44	7.98	0.46	7.84	0.60
12	7.89	8.33	-0.44	8.26	-0.37
13	8.11	8.08	0.03	8.03	0.08
15	7.92	7.96	-0.04	7.90	0.02
16	8.48	7.95	0.53	9.67	0.52
17	7.85	8.43	-0.58	19.3	-0.45
18	8.17	8.64	-0.47	8.19	-0.02
19	8.49	7.94	0.55	8.03	0.46
21	6.92	7.07	-0.15	6.37	0.55
22	5.57	6.14	-0.57	6.27	-0.70
23	6.02	6.17	-0.15	5.90	0.12
24	5.19	5.78	-0.59	5.96	-0.77
25	5.20	5.67	-0.47	6.10	-0.90
26	6.75	6.67	0.08	6.10	0.65
27	6.83	6.64	0.19	6.35	0.48
28	5.48	5.13	0.35	5.63	-0.15
29	4.62	4.76	-0.14	5.27	-0.65
30	4.49	5.27	-0.78	5.29	-0.80
31	5.29	5.42	-0.13	5.92	-0.63
32	4.85	5.01	-0.16	5.27	-0.42
33	5.28	5.14	0.14	4.83	0.45
34	5.39	5.31	0.08	5.19	0.20
35	5.17	5.30	-0.13	5.26	-0.09
36	5.10	4.99	0.11	5.14	-0.04
37	5.40	5.19	0.21	5.17	0.23
39	6.51	6.67	-0.16	6.64	-0.13
40	6.32	6.19	0.13	6.00	0.32
41	6.17	6.22	-0.05	6.11	0.06
42	6.62	6.59	0.03	6.28	0.34
43	5.91	6.61	-0.70	6.32	-0.41
44	7.03	6.72	0.31	6.77	0.26
45	5.95	6.65	-0.70	6.33	-0.38
46	6.67	6.52	0.15	6.98	-0.31
49	6.48	6.12	0.36	6.53	-0.05
50	6.83	7.59	-0.76	6.78	0.05
51	7.23	7.44	-0.21	6.95	0.28
52	7.89	6.93	0.96	7.40	0.49
54	7.55	6.69	0.86	6.77	0.78
55	5.96	5.99	-0.03	6.68	-0.72
56	6.70	6.91	-0.21	7.21	-0.51

SYBYL. Five different properties were used in CoMSIA studies, which are steric, electrostatic, hydrophobic, donor and acceptor, based on which similarity indices between a probe atom and compound were calculated. The probe atom with 1Å radius, +1 charge and +1 for hydrophobicity was set at the intersections of the lattice.

Molecular Docking Studies

Table 3: Experimental, predicted and residual values test set compounds of CoMFA, CoMSIA study

S. No	pIC_{50}	CoMFA		CoMSIA	
		Predicted	Residual	Predicted	Residual
6	7.74	8.60	-0.86	8.48	-0.74
10	7.31	8.05	-0.74	8.04	-0.73
11	7.41	8.07	-0.66	8.25	-0.84
14	7.24	7.95	-0.71	7.86	-0.62
20	7.28	8.25	-0.97	8.03	-0.75
38	6.30	6.78	-0.48	7.02	-0.72
47	5.78	6.71	-0.93	6.58	-0.80
48	5.82	6.64	-0.82	5.92	-0.10
53	6.44	5.80	0.64	6.28	0.16

Molecular docking studies were performed using Autodock 4.2[12] to calculate possible binding modes, screening and validation for all prenylated flavonoid derivatives. Default parameters were used in present study. All the molecules were docked into the binding site of a crystal structure of "Akt1 with AMP-PNP" (PDB id: 4EKK)[13] with 2.8Å resolution to provide the interaction between the receptor and the ligand. All the molecules were docked into the binding site of protein 4EKK using Autodock module, which uses genetic algorithm for generating protein-ligand interactions and molecules from the smaller fragments in the cavity of the receptor site. Grid was created, x, y, z (10.605 13.272 39.863 for 4EKK) coordinates of Glu341 was selected.

RESULTS AND DISCUSSION

CoMFA and CoMSIA

CoMFA and CoMSIA methods were applied to derive 3D-QSAR models for prenylated flavonoid derivatives as PKB/AKT1 inhibitors. The statistical results of CoMFA and CoMSIA analysis are summarized in Table 1. Best predictions were obtained with CoMFA standard model involving q^2 = 0.880, r^2 = 0.973, SEE =0.225, r^2cv = 0.883 and F-value =293.248 with number of components as 5 and column filtering 2.0 kcal/mol. In CoMSIA, the standard model predictions obtained are q^2 = 0.906, r^2 = 0.991, SEE =0.134, r^2cv = 0.910 and F-value =700.295 with number of components as 6 and column filtering 1.0 kcal/mol selected for CoMSIA. CoMSIA results show a higher predictive ability for prenylated flavonoid derivatives against PKB/AKT1 on comparison with the CoMFA results. Biological activities, predicted and residual values of both training set and test set compounds used in CoMFA and CoMSIA are shown in table 1 and table 2 respectively. The table 1 shows the results of relative contributions for CoMFA and CoMSIA methods. 55.3% steric contribution was observed for steric, and 49.7% field contribution was observed for electrostatic in CoMFA, where in CoMSIA, the observed contributions for steric, electrostatic, hydrophobic, donor and acceptor properties are 9.2%, 23.1%, 15.7%, 32.3% and 19.7% respectively. Electrostatic property is the main contributor in CoMSIA analysis. The affinities between experimental and calculated values of the training set and

Table 4: Structure of compounds used in CoMFA and CoMSIA studies

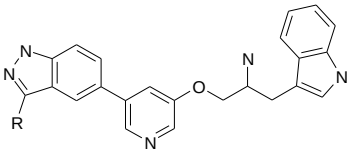

1. R=CF3
2. R=NH2
3. R=Cyclopropyl
4. R=H
5. R=Phenyl

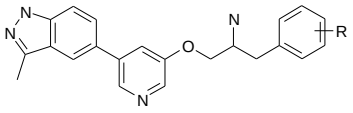

7. R=3F, 5CF3, 8. R=4CF3, 9. R=3F, 4Cl, 12. R=3,4-OCF2CF2O, 13. R=5F-2-OMe,15. R=2F, 4CF3,16. R=3-OCF3, 17. R=2,3-OCF2O, 18.

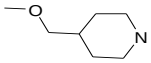

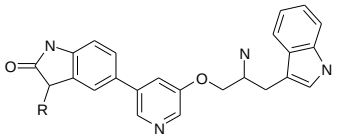

19. R=H

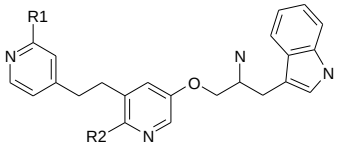

21. R1=NH2, R2=H
22. R1=OMe, R2=H
23. R1=H, R2=NO2
24. Phenyloxy, R2=H
25. R1=Benzylthio, R2=H
26. R1=NHCH3, R2=H
27. R1=NHCH2C6H6, R2=H
28. R1=Indol-1yl, R2=H

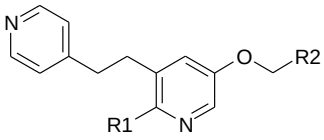

29. R1=H, R2=

30. R1=H, R2=

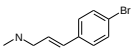

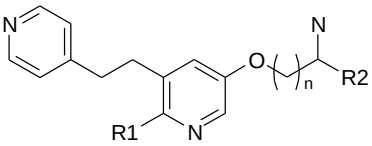

31. R1=H, R2=H(n=1)
32. R1=H, R2=H (n=2)
33. R1=Cl, R2=H (n=1)
34. R1=Cl, R2= benzyl, (n=1)
35 R1=H, R2=diphenylmethyl (n=1)
36. R1=H, R2=phenylethyl (n=1)
37. R1=H, R2=phenylmethoxymethyl

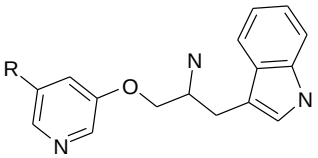

39. R=

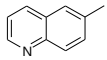

40. R=

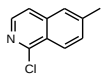

41. R=

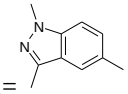

42. R=

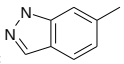

43. R=

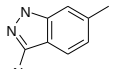

44. R=

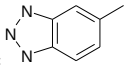

45. R=

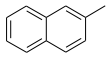

46. R=

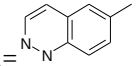

49 R=

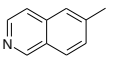

50. R=

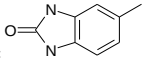

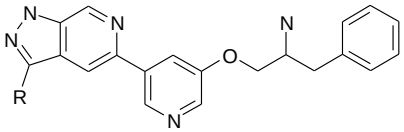

51. R=Me 52. R=Cl

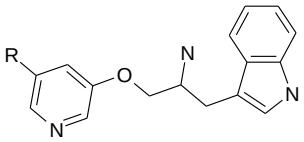

54. R=

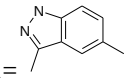

55.

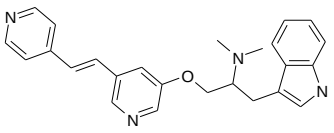

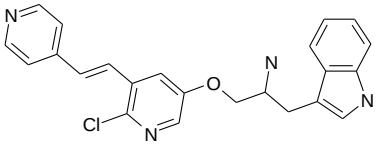

56.

the test set of CoMFA and CoMSIA models derived from non-cross-validated analysis are plotted in Figure 2(a) and 2(b). CoMSIA and the best CoMFA models were used to predict the inhibitory activities of the compounds in the test set.

Contour analysis

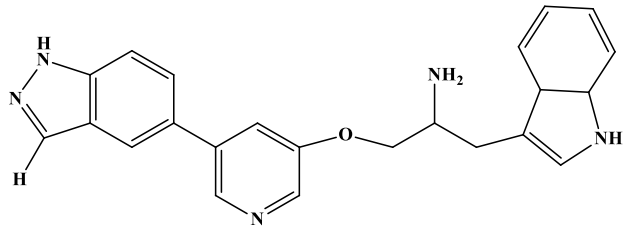

1-((5-(1H-indazol-5-yl)pyridin-3-yl)oxy)-3-(3a,7a-dihydro-1H-indol-3-yl)propan-2-amine (4)

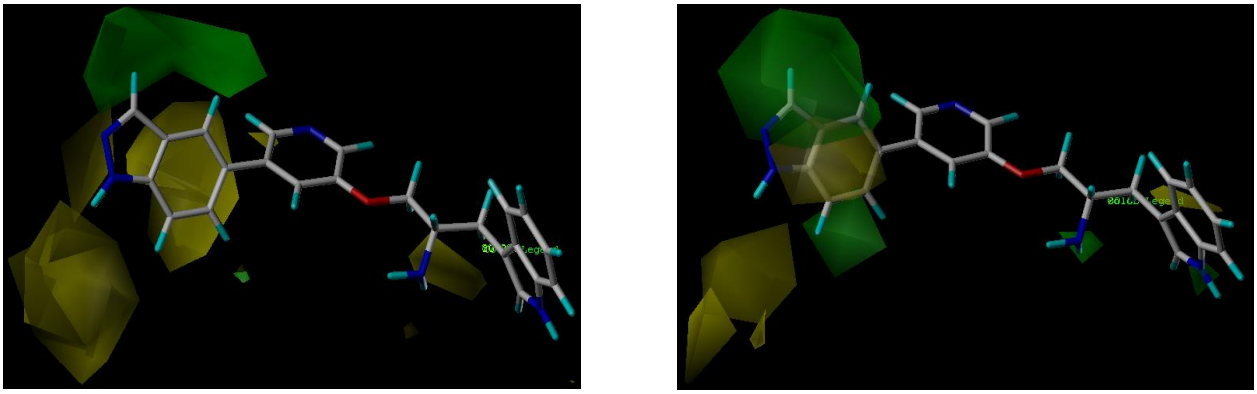

3(a) CoMFA 3(b) CoMSIA

Figure 3: The CoMFA and CoMSIA steric contour maps of 1-((5-(1H-indazol-5-yl) pyridin-3-yl) oxy)-3-(3a,7a-dihydro-1H-indol-3-yl) propan-2-amine (4)

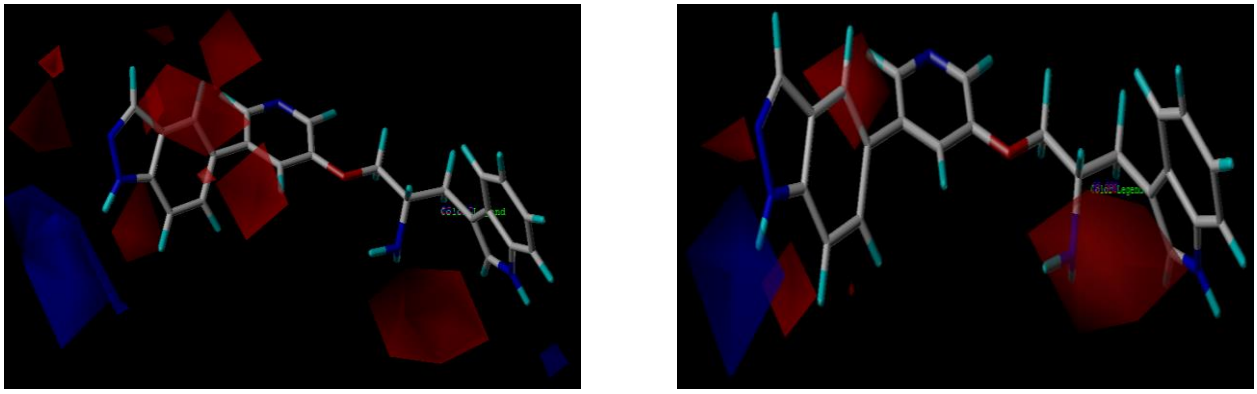

4(a) CoMFA 4(b) CoMSIA

Figure 4: CoMFA and CoMSIA electrostatic contour maps of 1-((5-(1H-indazol-5-yl)pyridin-3-yl)oxy)-3-(3a,7a-dihydro-1H-indol-3-yl)propan-2-amine (4)

The contour maps of 1-((5-(1H-indazol-5-yl) pyridin-3-yl) oxy)-3-(3a,7a-dihydro-1H-indol-3-yl) propan-2-amine (4) for CoMFA (steric and electrostatic) and CoMSIA (steric, electrostatic, donor, acceptor and hydrophobic) fields are represented in 3D contour plots and shown in Figures 3-5. The default parameters used in contour analysis by contribution are 80% favored region and 20% contribution for disfavored region. Structure of most active compound

Steric contour analysis

The steric field contour plots of CoMFA and CoMSIA for the most active compound 1-((5-(1H-indazol-5-yl) pyridin-3-yl) oxy)-3-(3a,7a-dihydro-1H-indol-3-yl) propan-2-amine (4) are depicted in Figure 3(a) and (b) respectively. CoMFA and CoMSIA steric maps are shown in green and yellow regions respectively. CoMFA steric maps for the most active compound 1-((5-(1H-indazol-5-yl) pyridin-3-yl) oxy)-3-(3a,7a-dihydro-1H-indol-3-yl) propan-2-amine (4) displayed a large green contour around to the 1-((5-(1H-indazol-5-yl regions on the other hand CoMSIA showed two large green contour around the 1-((5-(1H-indazol-5-yl position indicates more favorable regions where bulky substituents are expected to increase the activity. CoMFA steric maps also showed three large yellow contour above the 1-((5-(1H-indazol-5-yl region, whereas CoMSIA consists a two small yellow contours above and below the 1-((5-(1H-indazol-5-yl) position, suggests the disfavorable regions for bulky substituents.

Electrostatic contour analysis

The electrostatic contour plots of CoMFA and CoMSIA for the most active compound 1-((5-(1H-indazol-5-yl) pyridin-3-yl) oxy)-3-(3a,7a-dihydro-1H-indol-3-yl) propan-2-amine (4) are depicted in Figure 4(a) and (b) respectively. In CoMFA, the 1-((5-(1H-indazol-5-yl)pyridin-3-yl)oxy)-3-(3a,7a-dihydro-1H-indol-3-

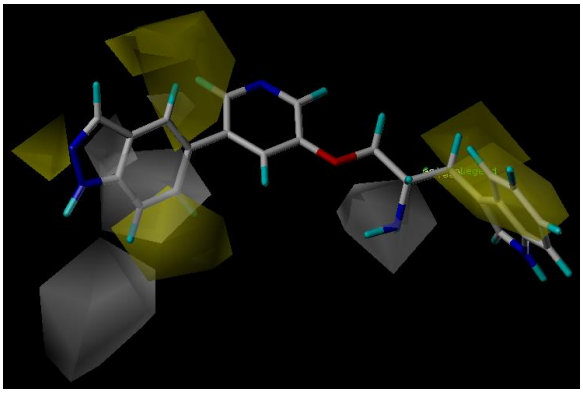

Figure 5(a): Hydrophobic contour maps of 1-((5-(1H-indazol-5-yl) pyridin-3-yl) oxy)-3-(3a,7a-dihydro-1H-indol-3-yl) propan-2-amine (4)

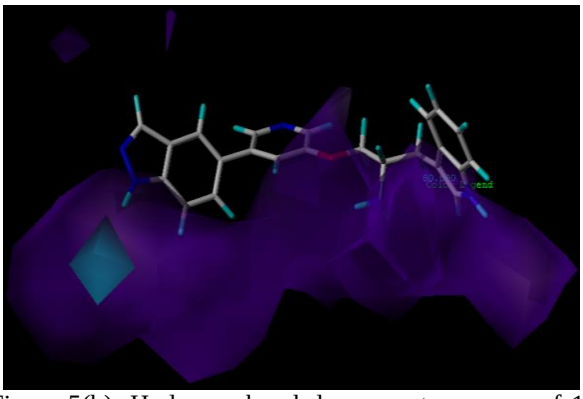

Figure 5(b): Hydrogen bond donor contour maps of 1-((5-(1H-indazol-5-yl) pyridin-3-yl) oxy)-3-(3a,7a-dihydro-1H-indol-3-yl) propan-2-amine (4)

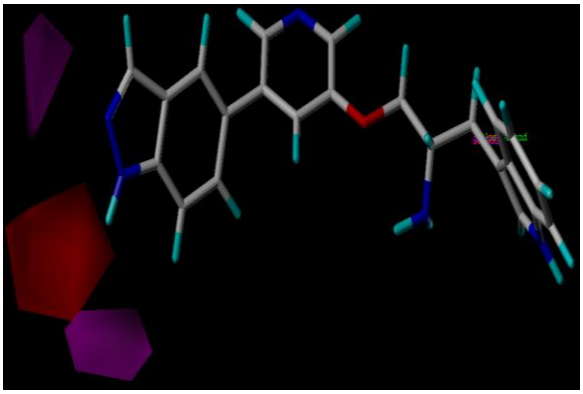

Figure 5(c): Hydrogen bond acceptor contour map of 1-((5-(1H-indazol-5-yl) pyridin-3-yl) oxy)-3-(3a,7a-dihydro-1H-indol-3-yl) propan-2-amine (4)

yl)propan-2-amine (4) showed a number of medium sized red contour aroud to the 1-((5-(1H-indazol-5-yl position and one medium-sized red contour nearer to propan-2-amine position where in CoMSIA three small red contours near to the 1-((5-(1H-indazol-5-yl position and a very large sized red contour below the 3-(3a,7a-dihydro-1H-indol-3-yl)propan-2-amine position envisage more favorable regions for -electron withdrawing groups. -I groups at these sites enhance biological activity. In CoMFA, and CoMSIA electrostatic contour plots also exhibits a large blue contour near to the 1-((5-(1H-indazol-5-yl position indicates more favorable regions where + I (electron donating) groups are expected to increase the activity

Hydrophobic contour analysis

The contour plots of CoMSIA hydrophobic fields for the most active compound 1-((5-(1H-indazol-5-yl) pyridin-3-yl) oxy)-3-(3a,7a-dihydro-1H-indol-3-yl) propan-2-amine (4) are depicted in Figure 5(a). Two large white contour present at 1-((5-(1H-indazol-5-yl) position, a medium-sized white contour at propan-2-amine position suggests favorable regions where hydrophilic substituents are increase the activity. The interaction of hydrophilic group may be more dominant for ligand binding. three large yellow contour present above, below the 1-((5-(1H-indazol-5-yl) pyridin and two medium sized yellow contour present at3-(3a,7a-dihydro-1H-indol-3-yl) above region indicates hydrophobic substituents increase the biological activity.

Hydrogen bond donor contour analysis

The hydrogen bond donor contour map of 1-((5-(1H-indazol-5-yl) pyridin-3-yl) oxy)-3-(3a,7a-dihydro-1H-indol-3-yl) propan-2-amine (4) shown in figure 5(b). A medium sized cyan contours present at 1-((5-(1H-indazol position indicates the favorable regions where the hydrogen bond donor groups increase the biological activity. There are two purple color contours present above the1-((5-(1H-indazol-5-yl) pyridin-3-yl, position and a very large purple color contours below the total molecule indicates unfavorable regions.

Hydrogen bond acceptor contour analysis

The hydrogen bond acceptor contour map of 1-((5-(1H-indazol-5-yl) pyridin-3-yl) oxy)-3-(3a,7a-dihydro-1H-indol-3-yl) propan-2-amine (4) shown in figure 5(c). Two medium sized magenta contour near to the 1-((5-(1H-indazol-5-yl) position indicates hydrogen-bond acceptor groups favorable at this positions. A small red contours below the 1-((5-(1H-indazol position suggests the disfavorable regions for hydrogen-bond acceptors.

Docking results

Molecular docking studies were performed using Autodock4.2. The results obtained by using molecular docking method disclosed the possible molecular interactions or orientation of flavonoid derivatives in the binding pocket of PDB id 4EKK. All the molecules were docked against the protein 4EKK. The most active compound showed a docking energy of -7.50 (3.18µm) kcal/mol for 4EKK and shows interactions with Val57 and Trp56. Least active compound shows energy of -6.87 (9.27 µm) Kcal/mol with 5 interactions. Figure 6(a) and (b) shows receptor ligand interactions for most and least active compounds for 4EKK.

CONCLUSION

The present work has carried out 3D-QSAR and molecular docking studies of some potent prenylated flavonoid derivatives of PKB/Akt1 inhibitors. Atom-based alignment was performed for all the 56 derivatives. The present 3D-QSAR model shows good statistical significance and good predictive ability. The 3D-QSAR model was generated using a training set of 47 molecules

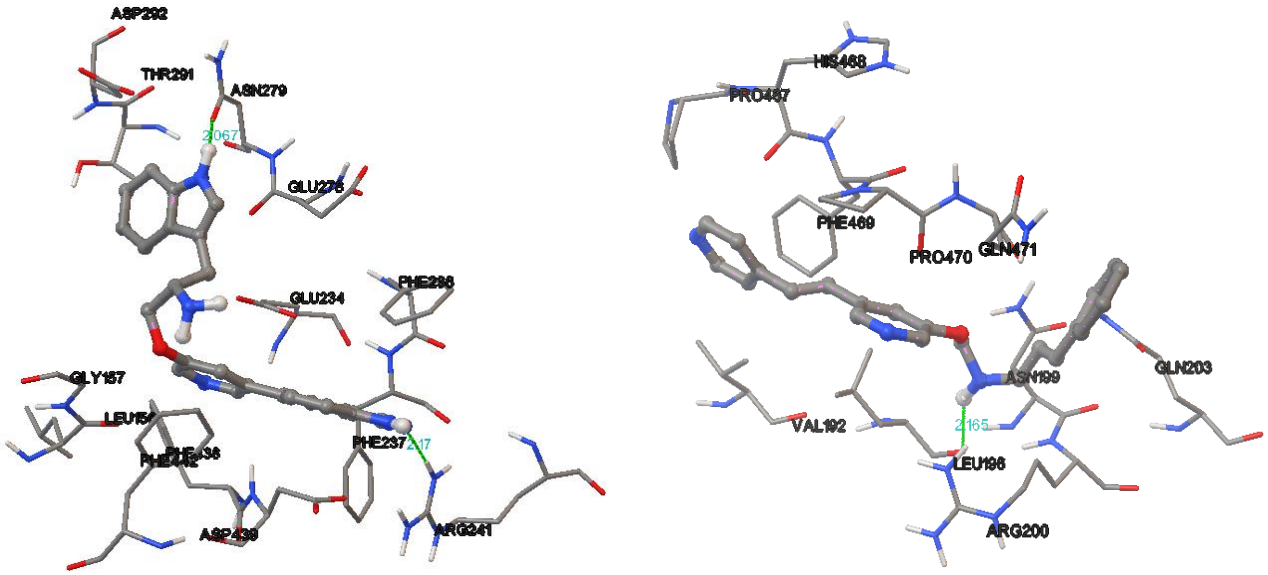

6(a) 6(b)

Figure 6(a): Docking interaction of most active compound and 6(b) Docking interaction of least active compound for 4EKK

and test set of nine molecules with q^2= 0.880 and 973 for CoMFA and q^2 = 906 and r^2 = 991. 3D-QSAR models for designing new PKB/AKT1 inhibitors for the treatment of cancer. Therefore, these models are useful in predicting the activity of new PKB/AKT1 inhibitors and can offer guidelines for the further modification of ligand design.

REFERENCES

1. Vivanco I, Sawyers CL. The phosphatidylinositol 3-Kinase AKT pathway in human cancer. Nat Rev Cancer. 2002, 2(7):489-501.
2. Vyas VK, Ghate M, Goel A. Pharmacophore modeling, virtual screening, docking and in silico ADMET analysis of protein kinase B (PKB β) inhibitors. J Mol Graph Model. 2013, 42:17-25.
3. Scheid MP, Woodgett JR. PKB/AKT: functional insights from genetic models. Nat Rev Mol Cell Biol. 2001, 2(10):760-8.
4. Kitamura T, Kitamura Y, Kuroda S, Hino Y, Ando M, Kotani K, Konishi H, Matsuzaki H, Kikkawa U, Ogawa W, Kasuga M. Insulin-induced phosphorylation and activation of cyclic nucleotide phosphodiesterase 3B by the serine-threonine kinase Akt. Mol Cell Biol. 1999, 19(9):6286-96.
5. Lawlor MA, Alessi DR. PKB/Akt: a key mediator of cell proliferation, survival and insulin responses? J Cell Sci. 2001, 114(Pt 16):2903-10.
6. Gunda SK, Kongaleti SF, Shaik M. Natural flavonoid derivatives as oral human epidermoid carcinoma cell inhibitors. Int J Comput Biol Drug Des. 2015;8(1):19-39.
7. Cramer III, R.D., Bunce, J.D., Patterson, D.E., Cross validation, bootstrapping, and partial least squares compared with multiple regression in conventional QSAR studies. Quant. Struct. Act. Relat. 1988, 7, 18–25.
8. Dong X, Zhou X, Jing H, Chen J, Liu T, Yang B, He Q, Hu Y. Pharmacophore identification, virtual screening and biological evaluation of prenylated flavonoids derivatives as PKB/Akt1 inhibitors. Eur J Med Chem. 2011, 46(12):5949-58.
9. Anugolu RK, Gunda SK, Mahmood S. 3D QSAR CoMFA/CoMSIA and docking studies on azole dione derivatives, as anti-cancer inhibitors. Int J Comput Biol Drug Des. 2012, 5(2):111-36.
10. Kumar SP, Jha PC, Jasrai YT, Pandya HA. The effect of various atomic partial charge schemes to elucidate consensus activity-correlating molecular regions: a test case of diverse QSAR models. J Biomol Struct Dyn. 2016, 34 (3):540-59.
11. Clark, M.; Cramer, R. D.; Van Opdenbosch, N. Validation of the general purpose tripos 5. 2 force field.J. Comput. Chem.1989, 10 (8), 982–1012.
12. Bhargava K, Nath R, Seth PK, Pant KK, Dixit RK. Molecular Docking studies of D2 Dopamine receptor with Risperidone derivatives. Bioinformation. 2014, 10(1):8-12.
13. http://www.rcsb.org/pdb/explore.do?structureId=4ekk